JOURNAL OF GUIDANCE, CONTROL, AND DYNAMICS
Vol. 23, No. 3, May–June 2000

Accuracy of the Global Positioning System-Derived Acceleration Vector

Mark L. Psiaki,* Steven P. Powell,† and Paul M. Kintner Jr.‡
Cornell University, Ithaca, New York 14853-7501

The accuracy with which acceleration can be determined from global positioning system (GPS) data has been investigated. This has been done to evaluate the possibility of using the GPS-derived acceleration as an attitude reference or in drop-sphere soundings of the upper atmosphere. The accuracy of the GPS acceleration signal has been investigated in two ways. One way has been to mathematically determine the acceleration error levels induced by receiver noise and by selective availability. The other way has been to use actual receiver data for receivers with known accelerations. Experimental acceleration accuracy of 0.009 g has been obtained at a 0.2 Hz bandwidth. The predicted achievable accuracy at a 1.6-Hz bandwidth is 0.03 g.

Nomenclature

A	= large coefficient matrix in least-squares estimation problem
$\boldsymbol{a}$	= acceleration vector or acceleration along line of sight to a GPS satellite
e_v	= selective availability range-rate error from the receiver to a given satellite
e_x	= selective availability range error from the receiver to a given satellite
f	= measured value of the integrated carrier phase
$\boldsymbol{g}$	= gravitational acceleration vector
J_2	= primary oblateness coefficient in spherical harmonic model of Earth's gravity field
N	= number of 0.001-s pseudorandom code periods in a least-squares problem
n_{IONO}	= carrier phase error due to ionospheric effects
n_{MP}	= carrier phase error due to multipath effects
n_{RCVR}	= carrier phase error due to receiver noise
n_{SA}	= carrier phase error due to selective availability
P_{SA}	= steady-state covariance matrix of the error vector $[e_x; e_v]$
$\boldsymbol{r}$	= position vector or range to a GPS satellite
R_{eq}	= equatorial radius of the Earth
t	= time
$\boldsymbol{v}$	= velocity vector or range rate to a GPS satellite
$w(t)$	= Gaussian white noise process with statistics $E\{w(t)\}=0$ and $E\{w(t)w(\tau)\}=\delta(t-\tau)$
$\boldsymbol{y}$	= sensed acceleration, inertial acceleration minus gravitational acceleration
Δt	= time interval between velocity outputs from a GPS receiver
λ	= L_1 carrier wavelength
μ	= geocentric gravitational constant
$\rho_{\text{SA}(n)}$	= autocorrelation of selective availability range error, $E\{e_x(t)e_x(t-0.001n)\}$
σ_a	= total standard deviation of the error in the GPS-derived LOS acceleration
$\sigma_{a(\text{RCVR})}$	= component of σ_a caused by receiver noise
$\sigma_{a(\text{SA})}$	= component of σ_a caused by selective availability
σ_{RCVR}	= standard deviation of n_{RCVR}
τ	= filtering time lag
τ_V	= time lag inherent to a GPS receiver's velocity calculation
$\Phi_{\text{SA}}(t)$	= state transition matrix for the error vector $[e_x; e_v]$
ϕ	= integrated carrier phase of the signal from a GPS satellite
$\boldsymbol{\omega}_E$	= Earth's rotational angular velocity vector

Subscripts

body	= vector in the body-fixed coordinate system
ECEF	= vector in the Earth-centered, Earth-fixed coordinate system with $+Z$ pointing to north pole and $+X$ pointing to equator at the Greenwich meridian
i	= i-axis component of vector in question
k, (k)	= occurring at time t_k

Superscripts

j	= having to do with GPS satellite j, such as the range to satellite j
$\hat{}$	= estimated value of the quantity

I. Introduction

THE global positioning system (GPS) is a space-based radio navigation system. It provides the ability to determine position and velocity anywhere on the globe. In autonomous mode, position is determined from time-of-flight measurements of the GPS signals, and velocity is determined from their Doppler shifts. The system consists of 24 satellites, a control segment, and a user segment. A stand-alone user can determine position, velocity, and universal time via passive reception of the signals from four or more satellites. For civilian users employing the standard positioning service, the stand-alone accuracy of this system is on the order of 100 m in horizontal position, 160 m in vertical position, 0.3 m/s in velocity, and 0.34 μs in time. Higher accuracies are available to military users who do not have to deal with deliberate signal degradation (selective availability) and for civilian users operating in a differential mode.[1]

Acceleration of a receiver can be deduced from the GPS signal. Acceleration is determined, effectively, by differentiation of the velocity. Real differentiators also must filter out high-frequency components to avoid excessive noise on the output. Therefore, the differentiated signal will have some phase lag behind the true acceleration.

Acceleration determination is not a typical use of the GPS system. Accelerations are used in inertial navigation systems only because they can be directly measured. They allow position and velocity to be deduced by integration. Position and velocity are already available from the GPS signals; thus, acceleration is not needed to derive them.

Received 27 October 1998; presented as Paper 99-4079 at the AIAA Guidance, Navigation, and Control Conference, Portland, OR, 9–11 August 1999; revision received 30 August 1999; accepted for publication 28 September 1999. Copyright © 2000 by the authors. Published by the American Institute of Aeronautics and Astronautics, Inc., with permission.

*Associate Professor, Sibley School of Mechanical and Aerospace Engineering. Associate Fellow AIAA.
†Research Support Specialist, School of Electrical Engineering.
‡Professor, School of Electrical Engineering.

GPS-derived accelerations are considered in the present paper because, given sufficient accuracy, they could be useful in two different applications. One application is to use the GPS-derived acceleration of a falling sphere to determine winds and density in the upper atmosphere. The other application is to use the GPS acceleration vector as an attitude reference during atmospheric flight.

A falling sphere experiment infers atmospheric parameters from the aerodynamic acceleration of the sphere.[2] The aerodynamic acceleration can be determined by measuring the inertial acceleration and subtracting out the gravitational acceleration. It would be very useful if a GPS receiver could be used to determine the inertial acceleration of a falling sphere to sufficient accuracy.

The GPS-derived acceleration vector could serve as an attitude reference if it were used in conjunction with a three-axis accelerometer. The basic concept is to determine the sensed acceleration vector $\boldsymbol{y}$ in two different coordinate systems and to use it as a reference to relate the attitude of one coordinate system to the attitude of the other. Such a single-vector measurement gives two-axes worth of attitude information.

The sensed acceleration vector is defined to be the output of a proof-mass accelerometer, that is, the inertial acceleration minus the gravitational acceleration. In a vehicle's body reference frame, vector $\boldsymbol{y}_{\text{body}}$ can be measured directly by a three-axis accelerometer. This same vector can be constructed in an Earth-fixed reference frame by using the outputs of a GPS receiver:

$$\begin{aligned}\boldsymbol{y}_{\text{ECEF}} &= \boldsymbol{a}_{\text{IN/ECEF}} - \boldsymbol{g}_{\text{ECEF}}(\boldsymbol{r}_{\text{ECEF}}) \\ &= \boldsymbol{a}_{\text{ECEF}} + 2\boldsymbol{\omega}_E \times \boldsymbol{v}_{\text{ECEF}} + \boldsymbol{\omega}_E \times (\boldsymbol{\omega}_E \times \boldsymbol{r}_{\text{ECEF}}) - \boldsymbol{g}_{\text{ECEF}}(\boldsymbol{r}_{\text{ECEF}})\end{aligned} \tag{1}$$

The position $\boldsymbol{r}_{\text{ECEF}}$ and the velocity $\boldsymbol{v}_{\text{ECEF}}$ come directly from the GPS receiver. The receiver's Earth-relative acceleration $\boldsymbol{a}_{\text{ECEF}}$ is determined by filtered differentiation of $\boldsymbol{v}_{\text{ECEF}}$ (or by an equivalent operation, as will be described). The gravity vector $\boldsymbol{g}_{\text{ECEF}}(\boldsymbol{r}_{\text{ECEF}})$ is determined from a gravity model.

The directions of the two vectors $\boldsymbol{y}_{\text{ECEF}}$ and $\boldsymbol{y}_{\text{body}}$ determine two of the three Euler rotation angles for the transformation from Earth-fixed coordinates to body coordinates. In an aircraft or a ship, these vectors nominally point toward nadir. In this case they provide a roll and pitch attitude reference, and the remaining unknown Euler angle is yaw. In the case of a turn, an aircraft loop, or almost any other maneuver, the sensed acceleration vector still provides two-axes worth of attitude information, but the two axes are not necessarily roll and pitch. The only situation in which this vector would fail to provide an attitude reference would be a free-fall maneuver, when $\boldsymbol{y}_{\text{ECEF}}$ and $\boldsymbol{y}_{\text{body}}$ are both vectors of zero length. This limitation precludes the use of this concept on a satellite, where free fall is the norm.

To get full three-axis attitude, roll, pitch, and yaw, an additional reference vector would be needed.[3] One possible additional reference vector is the Earth's magnetic field. Its use would require the addition of a magnetometer to the system. Another possibility is to use the aircraft velocity vector along with air data and an estimate of the wind vector; this is similar to what has been done in Ref. 4.

The goal of the present work is to determine the possible accuracy of GPS-derived acceleration for a stand-alone civilian receiver. The accuracy will be determined theoretically from models of selective availability (SA) and receiver noise. It will also be determined experimentally from tests in which the receiver's acceleration is known independently. (Note that SA is a deliberate degradation of the GPS signal's accuracy for non-U.S.-military users. It has been introduced to deny use of the full accuracy of the GPS system to adversaries of the United States. It is normally the principal source of position and velocity errors for an autonomous civilian receiver.)

GPS-derived accelerations have already been considered in two contexts. One is that of airborne gravimetry. References 5 and 6 are examples of work in this area. Airborne gravimetry requires acceleration accuracies on the order of 10^{-6} g to accurately map out the gravity field by differencing the GPS-derived inertial acceleration with the output of a proof-mass accelerometer. The required accuracies are achieved by using differential GPS and by averaging the results over time periods on the order of 1 min. The resulting long delay times are unacceptable for purposes of drop-sphere experiments or real-time attitude determination, but then again, the levels of error achieved by these techniques are smaller than would be needed for these applications.

Other works have considered the real-time computation of the GPS-derived acceleration of a stand-alone civilian receiver.[4,7] In fact, Ref. 4 also considers the possibility of using the acceleration to determine attitude-like quantities, quantities which it calls "pseudo-attitude." The contribution of the current work is the following: it is the first to determine and report the accuracy with which GPS acceleration can be determined in real time.

The body of this paper discusses GPS acceleration and its accuracy in three sections. Section II develops a real-time differentiator for acceleration determination, presents some GPS noise models, and uses the noise models to analyze the differentiator's acceleration accuracy. Section III presents experimental acceleration accuracy results. Section IV summarizes the analytical and experimental acceleration accuracy results and briefly discusses the suitability of GPS-derived acceleration accuracies for the drop-sphere and attitude-determination applications. Section V concludes the work.

II. Mechanism for GPS Acceleration Determination and an Analysis of its Accuracy

To determine acceleration from the GPS signal it is necessary to differentiate measured signals. Differentiation tends to amplify noise. Therefore, the differentiator must include filtering so as to limit the noise effects on the derived acceleration.

There are a number of noise sources in the GPS signal. One source is receiver noise, which includes thermal noise and digitization error. Another error source is SA. Three other sources are multipath effects, ionospheric effects, and vehicle dynamics. Multipath refers to the reception of reflected signals. The GPS signal and receiver antennas are circularly polarized to minimize multipath effects, but they still can cause significant system errors. Ionospheric effects arise from signal propagation delays that occur in the ionosphere. Dynamic motion of the user's receiver will cause acceleration errors if the acceleration has time variations with significant high-frequency content. This error is caused by the filtering that must be used in the differentiator to mitigate the effects of other noise sources.

Batch Differentiator to Determine GPS Line-of-Sight Acceleration

The GPS acceleration calculation starts with a determination of the acceleration of the line-of-sight (LOS) vector from the receiver to a given GPS satellite. The LOS accelerations to four or more GPS satellites can then be combined with satellite ephemerides to simultaneously estimate the vehicle's acceleration vector and the frequency drift rate of the receiver clock.

The LOS acceleration is determined from the rate of change of the Doppler shift of the GPS signal in question. The fundamental measurement that is made by the GPS receiver is the integrated carrier phase of the signal from the jth GPS satellite, $\phi^j(t)$. It is the electrical phase of the difference between the GPS L_1 carrier signal and that of a 1575.42-MHz reference oscillator onboard the receiver. To determine the LOS acceleration, it is necessary to take the second derivative of the integrated carrier phase and then scale it by the carrier wavelength.

One way to take this second derivative is to solve a batch estimation problem of the form

$$\lambda \begin{bmatrix} \phi^j(t_{k-N+1}) \\ \phi^j(t_{k-N+2}) \\ \phi^j(t_{k-N+3}) \\ \vdots \\ \phi^j(t_k) \end{bmatrix} = \begin{bmatrix} 1 & (t_{k-N+1}-t_k) & \frac{1}{2}(t_{k-N+1}-t_k)^2 \\ 1 & (t_{k-N+2}-t_k) & \frac{1}{2}(t_{k-N+2}-t_k)^2 \\ 1 & (t_{k-N+3}-t_k) & \frac{1}{2}(t_{k-N+3}-t_k)^2 \\ \vdots & \vdots & \vdots \\ 1 & 0 & 0 \end{bmatrix} \times \begin{bmatrix} \Delta r_k^j \\ v_k^j \\ a_k^j \end{bmatrix} = A \begin{bmatrix} \Delta r_k^j \\ v_k^j \\ a_k^j \end{bmatrix} \tag{2}$$

for the delta range, LOS velocity, and LOS acceleration to GPS satellite j. The A matrix on the extreme right-hand side of Eq. (2) is a short-hand notation for the large $N \times 3$ matrix that appears in the middle expression of the equation. If λ is expressed in meters per cycle, ϕ in cycles, and t in seconds, then the LOS acceleration a_k^j will be expressed in meters per second squared. Note that $\lambda = 0.19$ m/cycle for the civilian L_1 GPS signal.

The batch estimation problem in Eq. (2) can be solved via a least-squares technique. The solution takes the form

$$\begin{bmatrix} \Delta\hat{r}_k^j \\ \hat{v}_k^j \\ \hat{a}_k^j \end{bmatrix} = (A^T A)^{-1} A^T \left\{ \lambda \begin{bmatrix} \phi^j(t_{k-N+1}) \\ \phi^j(t_{k-N+2}) \\ \phi^j(t_{k-N+3}) \\ \vdots \\ \phi^j(t_k) \end{bmatrix} \right\} \tag{3}$$

This batch estimate of the LOS acceleration $\hat{a}_k^j$ amounts to a filtered second derivative of the integrated carrier phase. The estimator assumes that the acceleration is constant over the batch interval from t_{k-N+1} to t_k. If the acceleration is time varying at a frequency that is low compared to $1/(t_k - t_{k-N+1})$ rad/s, then, effectively, there is a time delay between the actual acceleration and the $\hat{a}_k^j$ output. This time lag is $\tau = (t_k - t_{k-N+1})/2 \cong 0.0005N$ s.

Other differentiator implementations can be used to determine the acceleration of a GPS LOS vector. In choosing a differentiation scheme, one must be careful that the differentiator efficiently filters out noise. A poor choice of differentiator can result in a greatly increased noise level in the estimated acceleration. This particular implementation has been chosen for study for two reasons. First, it is relatively simple to understand. Second, it closely approximates an optimal Kalman filter in the amount of noise that it transmits for a given effective time lag.

One might question the use of a double-differentiation operation. On first glance, it might seem wiser to single differentiate the receiver's Doppler shift. Effectively, these are identical operations. The Doppler shift is not a fundamental measurement of a GPS receiver. A receiver's Doppler shift computation, which is normally carried out as part of a phase-locked loop, amounts to a differentiation of the integrated carrier phase measurement. In recognition of this, the present analysis uses a receiver's fundamental measurements.

Noise Models

The integrated carrier phase signals used in Eqs. (2) and (3) will be corrupted by noise. The measured value of the integrated carrier phase will be used in place of ϕ in Eq. (3). Its relationship to $\phi^j(t_k)$ is

$$f_k^j = \phi^j(t_k) + n_{\mathrm{RCVR}(k)} + n_{\mathrm{SA}(k)} + n_{\mathrm{MP}(k)} + n_{\mathrm{IONO}(k)} \tag{4}$$

The noise terms n_{RCVR}, n_{SA}, n_{MP}, and n_{IONO} affect the accuracy of the GPS-derived acceleration. The effects of the receiver noise and of the SA noise can be modeled and analyzed. The effects of multipath noise and ionospheric noise are too hard to model; they will be neglected. Thus, the resulting accuracy analysis will be optimistic in terms of the effects on the derived acceleration of multipath and ionospheric errors.

The receiver noise is modeled as a Gaussian, zero-mean, discrete-time, white-noise random process. Its statistical model is $E\{n_{\mathrm{RCVR}(k)}\} = 0$ and $E\{n_{\mathrm{RCVR}(k)} n_{\mathrm{RCVR}(l)}\} = \sigma_{\mathrm{RCVR}}^2 \delta_{kl}$. The receiver noise is statistically uncorrelated with the SA noise; that is, $E\{n_{\mathrm{RCVR}(k)} n_{\mathrm{SA}(l)}\} = 0$.

The SA model is a correlated random noise model. A second-order Markov process can be used to model this error source[8]

$$\begin{bmatrix} \dot{e}_x \\ \dot{e}_v \end{bmatrix} = \begin{bmatrix} 0 & 1 \\ -0.000144 & -0.0170 \end{bmatrix} \begin{bmatrix} e_x \\ e_v \end{bmatrix} + \begin{bmatrix} 0 \\ 0.0508 \end{bmatrix} w \tag{5a}$$

$$n_{\mathrm{SA}(k)} = e_x(t_k)/\lambda \tag{5b}$$

where e_x is in meters and e_v is in meters per second and where $w(t)$ is a white-noise process of unit intensity.

This model has been adopted as a standard for describing SA. It is known to produce velocity and acceleration error predictions that are noisier than the real SA effects.[8] Therefore, the results that will be derived using this model will probably be conservative; that is, they will probably show poorer accuracy than can actually be achieved by a real system.

Effects of Satellite Geometry

The effects of LOS acceleration errors on a vehicle's vector acceleration errors depend on satellite geometry. This geometry factor is summarized by a quantity known as the geometric dilution of precision (GDOP).[1] For modern receivers that have 10–12 channels, GDOP is often less than 3 under good satellite viewing conditions. Such low values of GDOP imply that per-axis acceleration error statistics will be on the order of the LOS acceleration error statistics. Therefore, the per-axis acceleration error statistics can be estimated by combining the per-channel range errors from Eq. (4) with the model of the batch differentiator in Eq. (3).

Calculation of Acceleration Error Statistics

The batch differentiator model in Eq. (3) and the noise models in Eqs. (4–5b) can be combined to yield predicted standard deviations of the receiver-noise-induced and SA-induced acceleration errors. The analysis neglects $n_{\mathrm{MP}(k)}$ and $n_{\mathrm{IONO}(k)}$ in Eq. (4). It uses f_n^j from Eq. (4) to replace $\phi^j(t_n)$ in Eq. (3). This is done for every value of n from $k - N + 1$ up to k. The modified version of Eq. (3) is then used to compute variances using standard techniques. The resulting acceleration variance is

$$\sigma_a^2 = [0 \quad 0 \quad 1](A^T A)^{-1} A^T \left\{ I\lambda^2 \sigma_{\mathrm{RCVR}}^2 + \begin{bmatrix} \rho_{\mathrm{SA}(0)} & \rho_{\mathrm{SA}(1)} & \cdots & \rho_{\mathrm{SA}(N-1)} \\ \rho_{\mathrm{SA}(1)} & \rho_{\mathrm{SA}(0)} & & \vdots \\ \vdots & & \ddots & \rho_{\mathrm{SA}(1)} \\ \rho_{\mathrm{SA}(N-1)} & \cdots & \rho_{\mathrm{SA}(1)} & \rho_{\mathrm{SA}(0)} \end{bmatrix} \right\} A(A^T A)^{-1} \begin{bmatrix} 0 \\ 0 \\ 1 \end{bmatrix} \tag{6}$$

This analysis assumes that all of the measurement sample times, $t_{k-N+1}, t_{k-N+2}, t_{k-N+3}, \ldots, t_k$, are equally spaced at 0.001-s intervals, which is a reasonable assumption.

The quantity $\rho_{\mathrm{SA}(n)}$ in Eq. (6) can be computed using the SA model in Eq. (5a). Suppose that P_{SA} is the solution to the following Lyapunov equation:

$$\begin{bmatrix} 0 & 1 \\ -0.000144 & -0.0170 \end{bmatrix} P_{\mathrm{SA}} + P_{\mathrm{SA}} \begin{bmatrix} 0 & 1 \\ -0.000144 & -0.0170 \end{bmatrix}^T = -\begin{bmatrix} 0 & 0 \\ 0 & (0.0508)^2 \end{bmatrix} \tag{7}$$

and that

$$\Phi_{\mathrm{SA}}(t) = \exp\left\{ \begin{bmatrix} 0 & 1 \\ -0.000144 & -0.0170 \end{bmatrix} t \right\} \tag{8}$$

Then

$$\rho_{\mathrm{SA}(n)} = [1 \quad 0]\Phi_{\mathrm{SA}}(0.001n) P_{\mathrm{SA}} \begin{bmatrix} 1 \\ 0 \end{bmatrix} \tag{9}$$

Predicted Acceleration Accuracy

The acceleration error standard deviation σ_a has been calculated as a function of the differentiator's time lag $\tau = 0.0005N$. Figure 1 presents a plot of σ_a (in g units) vs τ (in seconds). Also shown are the SA and receiver-noise components of σ_a. The receiver-noise component has been calculated based on the assumption that $\sigma_{\mathrm{RCVR}} = \frac{1}{36}$ cycle (10 electrical degrees of phase). This value is consistent with

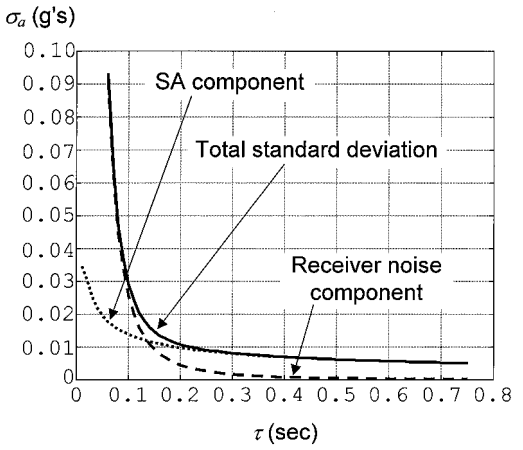

Fig. 1 Theoretical standard deviations of the GPS-derived acceleration as functions of the differentiator time lag.

experimental data from a GPS receiver that has 2-bit digitization of its down-converted RF signal and a coherent delay-locked loop for pseudorandom code tracking.

According to Fig. 1, SA noise dominates the acceleration error for differentiator time lags above $\tau = 0.13$ s, and receiver noise dominates at shorter time lags. It is possible to derive simple models of these two error standard deviations that are valid for $0.05 \text{ s} < \tau < 10$ s. These simple models are $\sigma_{a(\text{RCVR})} = 7.9 \times 10^{-4}/\tau^{2.5}$ and $\sigma_{a(\text{SA})} = 0.043/\tau^{0.5}$, where τ is expressed in seconds and both standard deviations are expressed in meters per second squared. Note that the $\sigma_{a(\text{RCVR})}$ formula can be rescaled for a receiver whose phase noise intensity is different from the value that has been assumed here ($\sigma_{\text{RCVR}} = \frac{1}{36}$ cycle).

This analysis indicates that reasonable acceleration accuracy can be had for differentiator time lags as low as $\tau = 0.1$ s. At this time lag, the error standard deviation is about 0.03 g. This time lag corresponds to an acceleration estimation bandwidth of approximately $1/(2\pi 0.1) = 1.6$ Hz. As bandwidth increases from this value, the acceleration accuracy degrades very rapidly due to the effects of receiver noise.

III. Experimental Tests of Acceleration Determination Accuracy

The achievable acceleration accuracy can be investigated experimentally by placing a GPS receiver on a platform whose acceleration is known by some independent means. The GPS data are used to derive acceleration, and this acceleration is compared to the independently known acceleration to evaluate the accuracy of the GPS technique. The results of such studies are reported in Refs. 5 and 6 for differential GPS systems. New tests were needed to find out the effects of SA on acceleration-determination accuracy for a standalone civilian receiver. Also, the new tests examined much shorter averaging periods to explore whether higher-bandwidth acceleration estimation will be feasible in the face of receiver noise.

Two studies have been conducted. One was for a GPS receiver that flew on a sounding rocket. That rocket flew out of the atmosphere so that there were no significant accelerations other than those produced by gravity. Therefore, it has been possible to deduce the correct system acceleration from a gravity model. The other study was for static receivers. The acceleration of a static receiver is known to be zero.

Sounding Rocket Tests of Acceleration Accuracy

The sounding rocket test used data from the NASA PHAZE II mission. This sounding rocket was launched to study the physics of the auroral zone. It flew to a maximum altitude of 945 km and stayed aloft for more than 1000 s. It carried a six-channel GPS receiver that output $\boldsymbol{r}_{\text{ECEF}}$ and $\boldsymbol{v}_{\text{ECEF}}$ approximately once every second.

The GPS acceleration accuracy for this mission has been evaluated by calculating $\boldsymbol{a}_{\text{ECEF}}$ in two ways and comparing the results. The first way was by finite differencing of the velocity data, $\boldsymbol{v}_{\text{ECEF}(1)}, \boldsymbol{v}_{\text{ECEF}(2)}, \boldsymbol{v}_{\text{ECEF}(3)}, \ldots, \boldsymbol{v}_{\text{ECEF}(N)}$:

$$\boldsymbol{a}_{\text{ECEF}}(t_k) = [\boldsymbol{v}_{\text{ECEF}(k)} - \boldsymbol{v}_{\text{ECEF}(k-1)}]/\Delta t_k \tag{10}$$

This constitutes the GPS-derived acceleration in this case.

Equation (10) represents a significant departure from the GPS differentiation mechanization of Eq. (3). Use of this variant differentiation mechanization has been necessitated by the form of the available data. The total time lag for this acceleration calculation includes the lag of the GPS velocity calculation, τ_V; the total lag is $\tau = (0.5\Delta t_k + \tau_V)$. The value of Δt_k is 1.0 s for most of the PHAZE II data set and $\tau_V = 0.25$ s for the receiver in question. Therefore, $\tau = 0.75$ s for most of the data set. Despite the difference between the acceleration calculation in Eq. (10) and that in Eq. (3), the theoretical acceleration error standard deviation is approximately the same function of τ as is shown in Fig. 1 for the range of τ values that occurred in the PHAZE II flight. This is true because SA errors dominate at such large time lags.

The truth value of $\boldsymbol{a}_{\text{ECEF}}$ was computed by using

$$\boldsymbol{a}_{\text{ECEF}} = \boldsymbol{g}(\boldsymbol{r}_{\text{ECEF}}) - 2\boldsymbol{\omega}_E \times \boldsymbol{v}_{\text{ECEF}} - \boldsymbol{\omega}_E \times (\boldsymbol{\omega}_E \times \boldsymbol{r}_{\text{ECEF}}) \tag{11}$$

which assumes that the rocket's inertial acceleration was due only to gravity. This assumption was analyzed and found to be reasonable for the part of the flight when the boosters were spent and the rocket was well outside of the sensible atmosphere, above 160 km. During this flight phase, the predicted errors caused by this assumption are orders of magnitude smaller than the expected errors in the time-differentiated GPS velocity signal.

The $\boldsymbol{r}_{\text{ECEF}}$ and $\boldsymbol{v}_{\text{ECEF}}$ values that have been used in Eq. (11) are those from the GPS receiver. Although these values are noisy, the effect of their errors on the truth value of $\boldsymbol{a}_{\text{ECEF}}$ is negligible compared to the expected errors in the finite difference acceleration.

The gravity model that was used in Eq. (11) included the $-\mu/r^2$ central force term and the J_2 oblateness effects:

$$\begin{aligned}\boldsymbol{g}(\boldsymbol{r}_{\text{ECEF}}) = {} & -\boldsymbol{r}_{\text{ECEF}} \left\{\frac{\mu}{\|\boldsymbol{r}_{\text{ECEF}}\|^3}\right\} \left\{1 - 4.5 J_2 \left[\frac{R_{eq}}{\|\boldsymbol{r}_{\text{ECEF}}\|}\right]^2 \left[\left(\frac{(\boldsymbol{r}_{\text{ECEF}})_z}{\|\boldsymbol{r}_{\text{ECEF}}\|}\right)^2 - \frac{1}{3}\right]\right\} \\ & + 3 J_2 \left\{\frac{\mu}{\|\boldsymbol{r}_{\text{ECEF}}\|}\right\} \left\{\frac{R_{eq}}{\|\boldsymbol{r}_{\text{ECEF}}\|}\right\}^2 \left\{\frac{(\boldsymbol{r}_{\text{ECEF}})_z}{\|\boldsymbol{r}_{\text{ECEF}}\|^4}\right\} \\ & \times \begin{bmatrix} (\boldsymbol{r}_{\text{ECEF}})_x (\boldsymbol{r}_{\text{ECEF}})_z \\ (\boldsymbol{r}_{\text{ECEF}})_y (\boldsymbol{r}_{\text{ECEF}})_z \\ -\left\{(\boldsymbol{r}_{\text{ECEF}})_x^2 + (\boldsymbol{r}_{\text{ECEF}})_y^2\right\} \end{bmatrix}\end{aligned} \tag{12}$$

The J_2-induced acceleration magnitude is on the order of the expected finite difference GPS acceleration errors. This effect had to be included in the truth model to make its accuracy better than that of the data that were being evaluated.

The acceleration results for this case are shown in Figs. 2–4. Figures 2–4 show the GPS-derived values $\boldsymbol{a}_{\text{ECEF}}(t_k)$ at the intersample times $0.5[t_k + t_{k-1}]$. This has been done to remove the effects of the Eq. (10) differentiator delay from the present discussion. As can be seen from Figs. 2–4, the truth and GPS-derived curves fall on top of each other. The only noticeable difference is the high-frequency noise in the GPS-derived acceleration curves.

The curves in Figs. 2–4 were originally generated with a truth acceleration whose gravity model did not include the J_2 Earth oblateness terms. In these original curves there was a noticeable low-frequency error between the theoretical and experimental acceleration curves. That error was eliminated by inclusion of the J_2 terms. Thus, the GPS-derived accelerations are sensitive enough to see the J_2 effect.

Except for the glitches that occur in the plots before $t = 200$ s, the differences between the theoretical curves and the experimental curves are less than 0.009 g, which is very good performance. The larger glitches that occur before $t = 200$ s are probably real

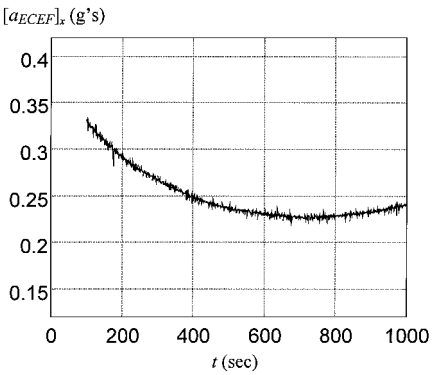

Fig. 2 GPS-derived and truth ECEF *x*-axis acceleration time histories for the PHAZE II sounding rocket.

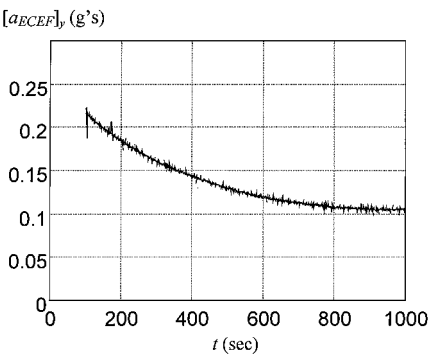

Fig. 3 GPS-derived and truth ECEF *y*-axis acceleration time histories for the PHAZE II sounding rocket.

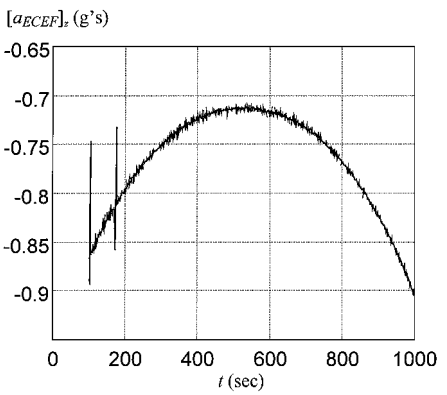

Fig. 4 GPS-derived and truth ECEF *z*-axis acceleration time histories for the PHAZE II sounding rocket.

accelerations, perhaps due to deployments or separations; notice how the large glitch at $t \cong 175$ s appears in Figs. 2–4. Alternatively, they may have been caused by changes to the set of GPS satellites that was used to generate the velocity solution.

These results have been compared to a theoretical accuracy model similar to that shown in Fig. 1, but modified to take into account the form of the GPS acceleration calculation in Eq. (10). As an example, Fig. 5 plots the time history of the differences between the GPS-derived values and the truth values of the z component of $\boldsymbol{a}_{\text{ECEF}}$. It also plots the theoretical σ_a values as positive and negative curves. The σ_a limits vary with time because there are variations in the Δt_k sample intervals for this data set that cause variations in the effective τ. Note that a receiver thermal noise level of $\sigma_{\text{RCVR}} = \frac{1}{36}$ cycle has been assumed.

As can be seen in Fig. 5, the actual errors are mostly smaller in magnitude than the predicted theoretical standard deviations. This trend holds true for all three components of the acceleration. The ratios of the experimental error standard deviations to the theoretical σ_a values are 0.41, 0.36, and 0.51 for the respective acceleration

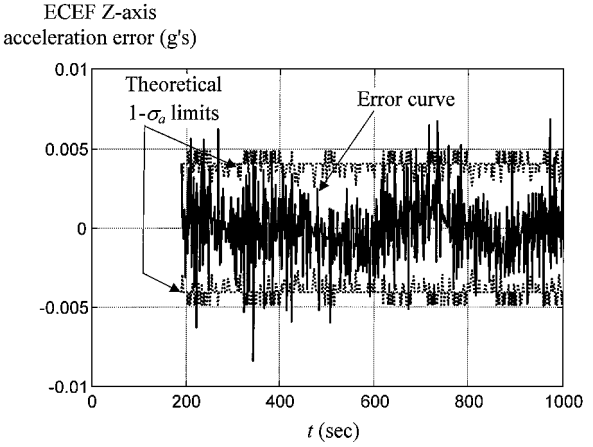

Fig. 5 Difference between GPS-derived and truth ECEF *z*-axis acceleration time histories for the PHAZE II sounding rocket.

components $[\boldsymbol{a}_{\text{ECEF}}]_x$, $[\boldsymbol{a}_{\text{ECEF}}]_y$, and $[\boldsymbol{a}_{\text{ECEF}}]_z$. Thus, the actual accuracy for this case is between two and three times better than that predicted by the theoretical SA/receiver-noise model. The SA effects dominate the theoretical value of σ_a for the large τ values that occur in this data set; therefore, the PHAZE II data support the assertion that the SA model in Eqs. (5a) and (5b) is conservative with regard to its predictions of SA effects on GPS-derived acceleration accuracy.

This level of accuracy is very good. The standard deviations are less than 0.0025 g per axis. This level of accuracy is due largely to the long effective differentiator time lag, $\tau = 0.75$ s, which averages out much of the noise. For shorter time lags the accuracy will degrade, but if these results are any indication, then actual performance will be somewhat better than that predicted by theoretical analyses such as the one that was used to produce Fig. 1.

Tests of Acceleration Accuracy Using Static Receivers

Static tests have been conducted using two different receivers, a 10-channel receiver, receiver A, and a 12-channel receiver, receiver B. Each receiver was connected to a stationary antenna mounted on the top of a building, and each produced outputs of pseudorange and Doppler shift at a sampling frequency of 1 Hz. These data were processed using a MATLAB® software package to determine $\boldsymbol{r}_{\text{ECEF}}$ and $\boldsymbol{v}_{\text{ECEF}}$. Afterward, the $\boldsymbol{v}_{\text{ECEF}}$ solutions were finite differenced to compute accelerations as in Eq. (10). These accelerations were compared to the known true Earth-relative acceleration, which was zero for these cases. Any nonzero Earth-relative acceleration constituted an acceleration error.

These tests include the receiver noise, SA, multipath, and ionospheric error sources, but not the vehicle dynamics error source. The multipath errors should be relatively low because of the antenna's location on the top of a tall building and because the antenna had a good ground plane. Therefore, these cases should have had lower acceleration errors than were found for the PHAZE II sounding rocket.

Receiver A produced very good acceleration results. Operating with 7 satellites and a GDOP of about 2.8, the standard deviations for the ECEF x, y, and z acceleration errors were 0.00035, 0.00119, and 0.00044 g, respectively. The maximum component acceleration error was 0.0037 g. As an example of these results, Fig. 6 shows a static receiver-A computed acceleration time history along the ECEF x axis. The expected per-axis standard deviation was $\sigma_a = 0.0048$ g at $\Delta t_k = 1$ s, $\tau_V = 0.25$ s, and $\sigma_{\text{RCVR}} = \frac{1}{36}$ cycle. (Note that the true value of τ_V was not readily available from the receiver manufacturer. The value 0.25 s has been used as a reasonable guess of τ_V. It is reasonable to use a guess of τ_V because σ_a is not strongly dependent on τ_V when the total $\tau = 0.75$ s.) Thus, the actual standard deviations were smaller than the theoretical values by factors ranging from 4.0 for the y acceleration component to 14 for the x component.

These results are better than for the GPS receiver data from the PHAZE II sounding rocket flight. It is not clear why this is so. Perhaps the lack of dynamic antenna motion caused receiver A to

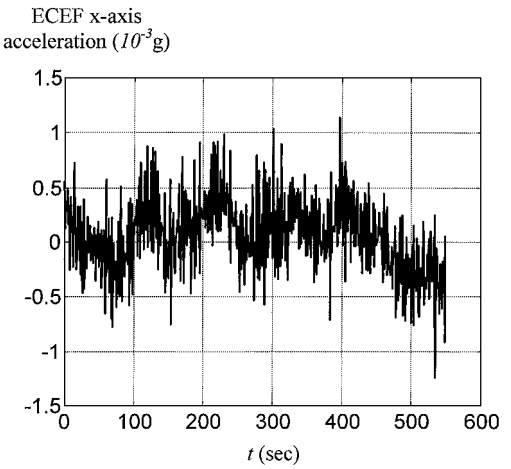

Fig. 6 ECEF *x*-axis component of the acceleration time history of a static antenna as determined from receiver A data.

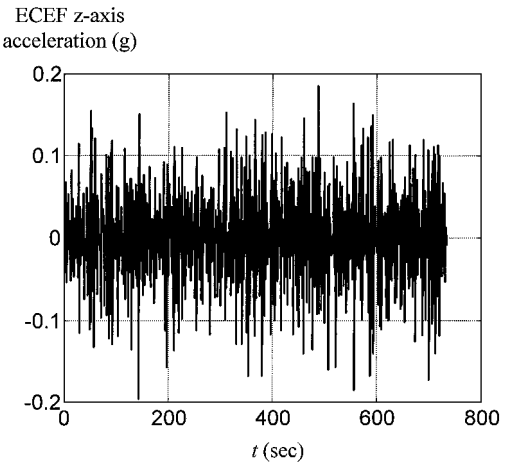

Fig. 7 ECEF *z*-axis component of the acceleration time history of a static antenna as determined from receiver B data.

perform better because it could not have had any time-lag-induced error.

Receiver B produced poor results. Operating under similar conditions to receiver A, receiver B's ECEF x-, y-, and z-axis acceleration error standard deviations were 0.028 g, 0.062 g, and 0.063 g, respectively. Figure 7 shows an example of this receiver's computed ECEF z-axis acceleration time history for a static antenna. These experimental standard deviations are between 5.8 and 13 times worse than the theoretical value $\sigma_a = 0.0048\ g$ that would apply if τ_V were 0.25 s. These accuracies are also much poorer than those that have been achieved by the PHAZE-II sounding rocket's receiver and by receiver A.

The poor results for receiver B highlight the importance of proper receiver design if one wants to determine acceleration from GPS signals. The receiver includes various feedback loops that allow it to lock onto a GPS satellite's signal and to track its pseudorandom code and Doppler shift. If these loops are designed poorly, then the resulting Doppler shift data will be very sensitive to receiver-generated noise. This is the case with receiver B. It uses a frequency-locked loop to track a GPS signal's Doppler shift. Its frequency-locked loop is designed to do a good job of maintaining lock, but it does a poor job of filtering out the 1000-Hz-bandwidth thermal noise that is present in its correlator's in-phase and quadrature accumulations. Stated differently, receiver B's equivalent velocity differentiation time constant τ_V is very small, approximately 0.01 s. Such a small filter time constant allows a large amount of receiver noise to pass to the velocity signal. This is a poor design if one wants to determine acceleration because it has the worst of everything: large noise because of a small τ_V, but long delays because of a large Δt_k. Receiver B's poor design effectively raises the level of the σ_a component curve that is labeled receiver noise component in Fig. 1. The curve gets increased by a factor of about 100 for values of τ near 0.5.

IV. Summary and Review of Accuracy Results

The accuracy of the GPS-derived acceleration has been investigated using two techniques, one theoretical and the other experimental. The theoretical results considered only the effects of receiver noise and SA. The experimental results considered two cases, that of a sounding rocket whose inertial acceleration was known to be that of the gravitational field and that of a static receiver whose Earth-relative acceleration was known to be zero.

The theoretical accuracy results are summarized by Fig. 1, which plots the acceleration noise standard deviation vs the acceleration calculation's time lag τ. The total theoretical error on this plot consists of two components whose root-sum-square value constitutes the total error. The receiver-noise component can be approximated by the formula $\sigma_{a(\mathrm{RCVR})} = 7.9 \times 10^{-4}/\tau^{2.5}$, and the SA component can be approximated as $\sigma_{a(\mathrm{SA})} = 0.043/\tau^{0.5}$. Thus, the total noise standard deviation can be approximated by the formula $\sigma_a = \{6.2 \times 10^{-7}/\tau^5 + 1.8 \times 10^{-3}/\tau\}^{0.5}$, where σ_a is in meters per second squared and τ is in seconds.

This theoretical accuracy result does not account for any dynamics error induced by motion of the user vehicle, nor does it account for multipath or ionospheric errors. The latter two error sources have not been analyzed. The dynamics errors for a given application can be estimated by considering the bandwidth of the user vehicle's acceleration spectrum. The dynamics-induced error will have two components. For acceleration signals with a bandwidth below $1/\tau$ rad/s, the dynamic error will come in the form of a phase lag of τ s. The remaining error will equal the total power of the acceleration signal that exists in the frequency band above $1/\tau$ rad/s. It is recommended that GPS-derived acceleration be used only in situations where this latter error source is negligible.

The experimental accuracy results test a limited portion of the curve in Fig. 1. The portion that has been tested is near $\tau = 0.75$ s ($\Delta t_k = 1.0$ s and $\tau_V = 0.25$ s). This is the portion of the curve that is dominated by SA errors. The results indicate that, for a well-designed receiver, Fig. 1 is conservative in this region. According to the experimental results, the actual error levels due to SA effects may be 2–4 times smaller.

It is not known whether multipath or ionospheric effects get averaged out to any significant degree when $\tau = 0.75$, as in the experimental data. If there is not much averaging, then the experimental data indicate that these two error sources are not significant in comparison to the SA effect.

Although the low-τ portion of Fig. 1 has not been experimentally verified, it is likely that Fig. 1 gives a good indication of the type of performance that will be achievable by a receiver whose phase-locked loop has been optimized for purposes of acceleration determination. This is true because Eq. (3) represents an optimized differentiator and because the receiver noise calculation that went into Fig. 1 used actual measured receiver noise levels in its determination of $\sigma_{a(\mathrm{RCVR})}$. For a receiver with a different level of phase noise than that assumed to produce Fig. 1, the receiver noise component curve in Fig. 1 can be rescaled to account for the receiver's different performance. Of course, this rescaling will be valid only if the receiver in question has a phase-locked loop that has been optimized or nearly optimized for the acceleration calculation.

These accuracy results can be used to evaluate the use of the GPS-derived acceleration for the two applications for which it has been proposed, the falling-sphere experiment in the upper atmosphere and the attitude determination application. In the falling sphere experiment, the goal is to resolve accelerations down to about 10^{-5}–$10^{-4}\ g$ with a τ of about 1.5 s. (This τ value yields a vertical resolution of 2 km at a vertical velocity of 0.7 km/s: 2 km $\cong 2 \times \tau \times 0.7$ km/s). Using the approximate theoretical formula for σ_a, one gets an error standard deviation of 0.004 g at this value of τ. Thus, a stand-alone system is inadequate for this task even if it is true that the SA model in Eqs. (5a) and (5b) overestimates acceleration errors by a factor of 4. If differential GPS were used, however, then the SA effects could be removed, and the expected noise level would be reduced to $\sigma_{a(\mathrm{RCVR})}\sqrt{2}$; the $\sqrt{2}$ factor comes in because of the use of a second

receiver. In this case, the theoretical standard deviation would be 4.1×10^{-5} g, which is clearly adequate for the task.

To evaluate accuracy for the attitude-determination application, the acceleration accuracy must be transformed into an expected attitude accuracy. As discussed in the introduction, two-axes worth of attitude could be deduced by comparing the sensed acceleration vector in the body reference frame with the sensed acceleration vector in an Earth-fixed reference frame. Recall that the sensed acceleration is what a proof-mass accelerometer would respond to, the difference between the inertial acceleration and the gravitational acceleration.

The nominal attitude reference accuracy can be computed by using the nominal length of the sensed acceleration vector. This vector will have a length of 1 g in normal flight of an airplane or in normal cruising of a ship. In turns, the sensed acceleration may be higher. Therefore, the nominal attitude accuracy will be $\sigma_a/9.81$ rad if σ_a is expressed in meters per second squared, and it will be just σ_a if σ_a is expressed in g units. Using Fig. 1 and assuming a delay of $\tau = 0.1$ s, the theoretical value of σ_a is 0.03 g. This translates into a 1.7-deg (0.03-rad) attitude reference accuracy. The bandwidth of this attitude reference signal is $1/\tau = 10$ rad/s, which equals 1.6 Hz. It is not practical to use a larger bandwidth than this because of the sharp increase in $\sigma_{a(\mathrm{RCVR})}$ that occurs when τ decreases below a value of 0.1 s.

V. Conclusions

A stand-alone civilian GPS receiver can be used to determine the acceleration of a moving vehicle to reasonable accuracy. The acceleration is determined, effectively, by double time differentiation of the GPS integrated carrier phase signal. Despite the usual noise amplification that accompanies differentiation, an experimental test with a sounding rocket yielded a worst-case acceleration error of less than 0.009 g for a 0.75-s differentiation time lag. This is remarkable when one considers that the signal contains high-frequency receiver noise and a deliberately introduced noise source known as SA.

A theoretical model of the acceleration error's dependence on filtering time lag has been used to predict an acceleration accuracy on the order of 0.03 g for a differentiator time lag of 0.10 s. This level of accuracy implies that it would be possible to use the GPS-derived acceleration vector as a two-axis attitude reference. This reference vector has a predicted $1 - \sigma$ attitude accuracy of 1.7 deg at a bandwidth of 1.6 Hz. For acceleration applications with more stringent accuracy requirements, lower bandwidths are required. For very high-accuracy requirements, the effects of SA must be removed, which requires a second, fixed receiver and operation in a differential mode.

References

[1] Hofmann-Wellenhof, B., Lichtenegger, H., and Collins, J., *GPS, Theory and Practice*, Springer–Verlag, New York, 1997, pp. 17, 18, 273–277, 321, 322.

[2] Philbrick, C. R., Schmidlin, F. J., Grossmann, K. U., Lange, G., Offermann, D., Baker, K. D., Krankowsky, D., and von Zhan. U., "Density and Temperature Structure over Northern Europe," *Journal of Atmospheric and Terrestrial Physics*, Vol. 47, Nos. 1–3, 1985, pp. 159–172.

[3] Bar-Itzhack, I. Y., "REQUEST: A Recursive QUEST Algorithm for Sequential Attitude Determination," *Journal of Guidance, Control, and Dynamics*, Vol. 19, No. 5, 1996, pp. 1034–1038.

[4] Kornfeld, R. P., Hansman, R. J., and Deyst, J. J., "Single Antenna GPS Based Aircraft Attitude Determination," *Proceedings of the Institute of Navigation National Technical Meeting*, 1998, pp. 345–354.

[5] Jekeli, C., and Garcia, R., "GPS Phase Accelerations for Moving-Base Vector Gravimetry," *Journal of Geodesy*, Vol. 71, 1997, pp. 630–639.

[6] Van Dierendonck, K. J., Cannon, M. E., Wei, M., and Schwarz, K. P., "Error Sources in GPS-Determined Acceleration for Airborne Gravimetry," *Proceedings of the Institute of Navigation National Technical Meeting*, 1994, pp. 811–820.

[7] Axelrad, P., and Brown, R. G., "GPS Navigation Algorithms," *Global Positioning System: Theory and Applications*, Vol. 1, edited by B. W. Parkinson and J. J. Spilker Jr., AIAA, Reston, VA, 1996, pp. 409–433.

[8] van Graas, F., and Braasch, M. S., "Selective Availability," *Global Positioning System: Theory and Applications*, Vol. I, edited by B. W. Parkinson and J. J. Spilker Jr., AIAA, Reston, VA, 1996, pp. 601–621.